AIAA 80-0701R

Coupled Bending-Torsion Flutter in a Supersonic Cascade

Oddvar Bendiksen*
University of Southern California, Los Angeles, Calif.
and
Peretz Friedmann†
University of California, Los Angeles, Calif.

An investigation of the effects of bending-torsion interaction on the flutter boundaries of a supersonic cascade is presented. The analysis is based on a computationally efficient solution of the unsteady supersonic flow using a dual integral equation formulation. Results indicate that bending-torsion coupling has a significant effect on the flutter boundaries, which agrees with results obtained previously by the authors for incompressible flow. Large variations in the critical interblade phase angle were sometimes observed. The results also indicate a potential instability in the bending mode even in the absence of strong shocks.

Nomenclature‡

a_0 = speed of sound in freestream
$C(\alpha), C(\tau)$ = cascade function in supersonic flow
$C_{M\alpha}$ = moment coefficient due to torsion, about midchord
d^2 = $s_1^2 - \beta^2 s_2^2$ = transformed slant distance
d_r, e_r, f_r = Mach wave reflection constants
$f_m(\alpha)$ = Fourier transform of mth blade reduced pressure jump
$F_0(\tau + \bar{k}M)$ = Fourier transform of pressure jump across zeroth blade
$G(\tau)$ = reduced kernel function in upwash integral equation
$H(\bar{x})$ = Heaviside unit step function
$j_n(z)$ = spherical Bessel function of the first kind, of order n
$J_n(z)$ = Bessel function, of order n
k = kM/β^2 = modified reduced frequency
k_F = $\omega_T b/U$ = critical reduced frequency for SDOF torsional flutter
M = U/a_0 = freestream Mach number
M_{ea}, M_{mc} = moment about elastic axis and midchord, respectively, per unit span, positive nose up
N_b = number of blades in rotor
N_r = number of Mach wave reflections
$p(x,y,t)$ = perturbation pressure
$[\tilde{p}_m(x')]$ = pressure jump amplitude $\tilde{p}_m(x',0^+) - \tilde{p}_m(x',0^-)$ across mth blade
$[\tilde{p}_0^s(\bar{x})]$ = nondimensionalized pressure jump amplitude across reference blade when Mach wave reflections are explicitly accounted for
p_n = coefficients in pressure jump expansion, in terms of Legendre polynomials
$P_n(\bar{x})$ = Legendre polynomial of degree n
s_1 = $s\sin\theta$ = stagger distance
s_2 = $s\cos\theta$ = cascade spacing normal to blade chord
v = perturbation velocity in y direction
x', y' = x,y coordinate system after a Prandtl-Glauert transformation
β = $\sqrt{M^2 - 1}$
$\Delta\epsilon$ = error vector
ρ_0 = freestream air density
$\phi_n(\bar{x}), \phi_n^*(\bar{x})$ = shape functions in supersonic cascade theory
$\psi(x,',y')$, $\psi_m(x',y')$ = reduced pressure functions for the cascade and mth blade, respectively
Ω = $\sigma + \bar{s}_1 \bar{k}M$ = reduced interblade phase angle

Superscripts and Subscripts

$(\bar{\ })$ = nondimensionalized quantity: lengths with respect to semichord b, velocities with respect to U, and pressures with respect to $\rho_0 U^2$; others, as defined; also denotes complex conjugate
$(\ )'$ = differentiation with respect to argument
$(\ )_{xx}, (\ )_{yy}$ = $[\partial^2(\ )/\partial x^2]$, $[\partial^2(\ )/\partial y^2]$, etc.
$(\tilde{\ })$ or $()_0$ = amplitude (dimensional) of a harmonic variable, except as noted

I. Introduction

THE prediction of the aeroelastic stability of fan and compressor rotors remains an important and difficult task in the development of modern aircraft turbofan engines. Although the theoretical and experimental understanding of this problem has improved considerably over the years, advances in the design technology of fuel efficient, high performance aircraft engines have negated much of the aeroelastic stability margins inherent in earlier designs. The size increase, coupled with the performance demands of modern high by-pass engines, have resulted in longer, thinner, and thus more flexible blading throughout the engine, with the design of a given blade representing a compromise between aerodynamic performance and structural integrity. As a result, aeroelastic stability has become a major concern, and is often the limiting design constraint in the case of the fan.

This paper is a continuation and extension of a previously published investigation[1] into the effects of coupling between the bending and torsional degrees of freedom on the flutter boundaries of typical cascades, representative of modern fan and compressor rotors. It was shown that the introduction of the bending degree of freedom has a pronounced effect on the flutter speed. Because of the basic nature of Ref. 1, Whitehead's[2] incompressible cascade theory was used to

Presented as Paper 80-0701 at AIAA/ASME/ASCE/AHS 21st Structures, Structural Dynamics and Materials Conference, Seattle, Wash., May 12-14, 1980; submitted May 14, 1980; revision received Dec. 9, 1980.

*Assistant Professor of Aerospace Engineering, Department of Aerospace Engineering. Member AIAA.

†Professor of Engineering and Applied Science, Mechanics and Structures Department. Associate Fellow AIAA.

‡Symbols not defined here are defined in Ref. 1.

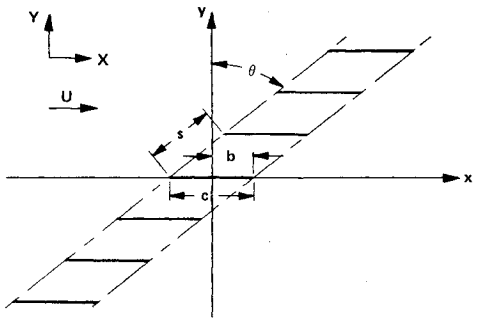

Fig. 1 Cascade geometry.

evaluate the unsteady aerodynamic forces, and no attempt was made to incorporate more advanced aerodynamic theories into the analysis.

The present paper has two objectives. First, an unsteady aerodynamic theory will be presented for the case of a cascade in supersonic relative flow with a subsonic leading-edge locus, which is the case of most practical interest in modern fans and compressors. Although several such theories[3-9] have been published in recent years, there was some concern about their suitability for incorporation into a general flutter analysis such as used in Ref. 1. The iteration procedure used to establish the flutter boundary requires that the calculation of the aerodynamic matrix be efficient and exhibit good convergence and numerical stability. Most methods permit the numerical accuracy to be increased, up to some limit characteristic of the procedure, at the expense of execution time. It is unfortunate that only Ref. 7 contains convergence data, since without such information computer execution times are meaningless. In view of these requirements, and due to the recent controversy regarding the existence of resonance phenomena,[8] it appeared advisable to derive an independent theory. Such a theory is also very useful in verifying the numerical reliability of the various existing methods.

The second objective is to systematically investigate the flutter problem for this type of supersonic cascade, and determine the effect of bending-torsion coupling on the flutter boundaries. It should be pointed out that previously published studies on supersonic cascades have been devoted to the unsteady aerodynamics; hence neither the single degree of freedom (SDOF) torsional nor the coupled bending-torsion case has been studied in a systematic manner from a flutter standpoint.

II. Structural Model

The real rotor is modeled as an infinite two-dimensional cascade of identical flat plate airfoils in a uniform upstream flow, as shown in Fig. 1. Following Ref. 1, the blades are modeled as equivalent sections with two degrees of freedom: bending displacement h normal to the chord, and torsional displacement α about the elastic axis. The airfoils are assumed to execute identical simple harmonic motion with an arbitrary, but constant phase angle σ between adjacent blades, and $\sigma = 2\pi n/N_b$; $n = 0, 1, 2, \ldots, N_b - 1$, in accordance with Lane's analysis[10] of admissible mode shapes for a tuned rotor. The derivation of the equation of motion and the formulation of the governing eigenvalue problem is given in Ref. 1.

III. Unsteady Supersonic Flow through a Cascade with Subsonic Leading-Edge Locus

The flow is assumed two dimensional and supersonic relative to the cascade, with a subsonic velocity component in the axial direction (normal to the leading-edge locus of the cascade). Assuming further that the flow is inviscid, isentropic, and irrotational, and that the vibration amplitudes are small, the governing field equation becomes the classical wave equation

$$(1-M^2)\psi_{xx} + \psi_{yy} - \frac{2M}{a_0}\psi_{xt} - \frac{1}{a_0^2}\psi_{tt} = 0 \tag{1}$$

where the coordinate system x,y is at rest with respect to the cascade, as shown in Fig. 1. The function ψ may be the velocity or acceleration potential, the pressure, or either of the disturbance velocities. It is convenient in the analysis that follows to work directly with the perturbation pressure, $p(x',y',t)$. Assume harmonic time dependence $p(x,y,t) = p(x,y)e^{i\omega t}$, and introduce the Prandtl-Glauert transformation

$$x' = x/\sqrt{M^2-1} = x/\beta, \quad y' = y \tag{2}$$

followed by the change of variable

$$\tilde{p}(x',y') = \psi(x',y')e^{-i\eta M x'} \tag{3}$$

where $\eta = \omega/(\beta a_0)$ is a constant. With these substitutions, Eq. (1) becomes

$$\psi_{x'x'} - \psi_{y'y'} + \eta^2\psi = 0 \tag{4}$$

which, following Miles,[11] will be referred to as the hyperbolic Helmholtz equation.

This equation must be solved subject to the following boundary conditions.

1) The flow must be tangential to the blades.

2) The pressure must be continuous everywhere off the blades (no shocks of finite strength).

3) Only outward propagating waves exist in the far field, away from the cascade (radiation condition). In the x',y' coordinate system, moving with the cascade at supersonic speed relative to the air, this means that there can be no upstream propagation of disturbances outside the Mach cone with vertex at the source of the disturbance.

The mathematical formulation of these boundary conditions requires careful considerations in view of the fact that the cascade is infinite and, therefore, extends into the far field. It should also be mentioned that weak shocks of finite strength are permissible within this formulation, but need not be considered in the unsteady solution. Within the framework of linearized theory, the effects due to finite but small thickness, camber, and mean angle of attack can be evaluated separately and superimposed; these solutions would in general contain weak shocks. Since in the unsteady solution it suffices to treat airfoils of zero thickness, zero camber, at zero mean angle of attack, no shocks of finite strength appear.

A. Derivation of the Dual Integral Equations

A detailed derivation of the governing dual integral equations is given in Ref. 12. Only a brief version will be attempted here. The analysis follows closely the analogous treatment of the subsonic case by Lane and Friedman,[13] although there are subtle differences due to the hyperbolic nature of Eq. (4), which necessitate special considerations in order to obtain convergence of certain integrals. Also, alternate derivations and justifications for some of the key steps have been provided.

The solution to the problem will be built up in two main steps. First, a solution for a *single* vibrating blade will be obtained in a form that satisfies the radiation condition and boundedness at infinity explicitly, but with the upwash boundary condition on the blade and the pressure continuity boundary condition off the blade left to be satisfied through the determination of an unknown function. These "fundamental" solutions will be then superimposed to obtain the complete solution for the cascade. Finally, the two remaining boundary conditions are enforced, leading to the final dual integral equations involving upwash and pressure jump.

It is shown in Ref. 12 that the fundamental solution required for the mth blade can be written as

$$\psi_m(x',y') = \frac{1}{2}\mathrm{sgn}(y'_m)\int_{-\infty}^{\infty} f_m(\alpha)\exp[i(\alpha x'_m - |y'_m|\sqrt{\alpha^2-\eta^2})]\mathrm{d}\alpha \quad (5)$$

where $f_m(\alpha)$ is an arbitrary function which must be determined from the remaining boundary conditions, that is, upwash on the blade and pressure continuity off the blade. The local blade coordinates x'_m and y'_m are given by

$$x'_m = x' - (ms_1)/\beta; \quad y'_m = y' - ms_2 \text{ for } m = 0, \pm 1, \pm 2, \ldots \quad (6)$$

It should be emphasized that the proper branch of the square root in Eq. (5) must be chosen. With a branch cut between $-\eta$ and $+\eta$, and the integration path passing along the bottom of the cut, the proper branch of the square root is the one that behaves as $+\alpha$ as $|\alpha| \to \infty$. The derivation of Eq. (5) involves the consideration of a singular eigenvalue problem involving the hyperbolic Helmholtz equation.

In order to ensure that the integral in Eq. (5) and subsequent integrals obtained exist, it becomes necessary to assume that α, ω, η, and k have small negative imaginary parts $-i\alpha_2$, $-i\omega_2$, $-i\eta_2$, and $-ik_2$, respectively, subject to the condition

$$0 < \alpha_2,\ \omega_2,\ \eta_2,\ k_2 \ll 1 \text{ and } 0 < \eta_2 < \alpha_2 \quad (7)$$

Ultimately the imaginary parts will be forced to zero, and this limit is implied in the analysis that follows.

The reduced pressure function ψ_m, as given by Eq. (5), is discontinuous across the line $y'_m = 0$, that is, across the x'_m axis represented by the mth blade and its extension to $\pm\infty$. The jump $[\psi_m]$ from the upper to the lower side of the line $y' = ms$ is

$$[\psi_m(x')] = \int_{-\infty}^{\infty} f_m(\alpha)e^{i\alpha x'_m}\mathrm{d}\alpha \quad (8)$$

which indicates that $[\psi_m]$ and f_m are Fourier transformations of each other.

The solution for the reduced pressure function for the complete cascade is obtained by summing the contributions from the individual blades,

$$\psi(x',y') = \sum_{m=-\infty}^{\infty} \psi_m(x',y') \quad (9)$$

Because of the assumptions made about the mode shapes, it follows that the pressure and velocity perturbations must obey the following periodicity conditions:

$$v[x' + (ms_1)/\beta,\ y' + ms_2] = v(x',0)e^{im\sigma} \quad (10)$$

where σ is the phase shift by which the $(m+1)$th blade leads the mth blade. Also,

$$[\tilde{p}_m(x')] = e^{im\sigma}[\tilde{p}_0(x'_m)] \quad (11)$$

$$[\psi_m(x')] = [\psi_0(x'_m)]e^{im\Omega} \quad (12)$$

$$f_m(\alpha) = e^{im\Omega}f_0(\alpha) \quad (13)$$

where

$$\Omega = \sigma + (\eta M s_1)/\beta \quad (14)$$

The function ψ can be related to the upwash v through the linearized momentum equation in the y direction. Integrating from $-\infty$ to x', and making use of the small negative imaginary part $-i\omega_2$ of ω to eliminate the boundary term at $-\infty$,

$$\tilde{v}(x',y') = -\frac{\beta e^{-i\omega\beta x'/U}}{\rho_0 U}\int_{-\infty}^{x'} \psi_{y'}e^{-i\eta\xi'/M}\mathrm{d}\xi' \quad (15)$$

Substituting for ψ from Eq. (9), making use of Eq. (5) and Eqs. (11-14), and reversing the order of integration, which is permissible as long as the order $0 < \eta_2 < \alpha_2 \ll 1$ is preserved in the limit $\omega_2, \eta_2, k_2, \alpha_2 \to 0^+$, the upwash integral equation for the reference blade can be written as

$$\tilde{v}(x',0) = \frac{\beta}{2\rho_0 U}e^{-i\eta x'M}\int_{-\infty}^{\infty} \frac{f_0(\alpha)\sqrt{\alpha^2-\eta^2}}{\alpha - (\eta/M)}C(\alpha)e^{i\alpha x'}\mathrm{d}\alpha \quad (16)$$

where

$$C(\alpha) = \sum_{m=-\infty}^{\infty} \exp[im(\Omega - \alpha s_1/\beta) - i|m|s_2\sqrt{\alpha^2-\eta^2}] \quad (17)$$

This series can be summed, provided one ties down the order relation, Eq. (7), by setting $\alpha_2 = M\eta_2$. Then

$$C(\alpha) = \frac{i\sin s_2\sqrt{\alpha^2-\eta^2}}{\cos s_2\sqrt{\alpha^2-\eta^2} - \cos[\Omega - (\alpha s_1/\beta)]} \quad (18)$$

Introducing dimensionless variables, the following integral equations are obtained for the unknown function $F_0(\tau)$ in terms of the upwash and the pressure jump across the zeroth blade and its extension $-\infty < \bar{x} < \infty$, $y = 0$:

$$\tilde{v}_0(\bar{x}) = \frac{i\beta}{2}e^{-i\bar{k}M\bar{x}}\int_{-\infty}^{\infty} G(\tau)F_0(\tau)e^{i\bar{x}\tau}\mathrm{d}\tau \quad (19)$$

$$[\tilde{p}_0(\bar{x})] = e^{-i\bar{k}M\bar{x}}\int_{-\infty}^{\infty} F_0(\tau)e^{i\bar{x}\tau}\mathrm{d}\tau \quad (20)$$

where

$$G(\tau) = \frac{\sqrt{\tau^2-\bar{k}^2}\sin\bar{s}_2\beta\sqrt{\tau^2-\bar{k}^2}}{[\tau - (\bar{k}/M)][\cos\bar{s}_2\beta\sqrt{\tau^2-\bar{k}^2} - \cos(\Omega - \tau\bar{s}_1)]} \quad (21)$$

In these equations, the limit $\omega_2 \to 0^+$ is implied, and in Eq. (19) the Cauchy principal value must be taken.

Thus, the solution of the problem has been reduced to the solution of the dual integral Eqs. (19) and (20) for the unknown function $F_0(\tau)$. In view of Eqs. (3) and (20), $F_0(\tau)$ is the Fourier transform of the pressure function ψ, and therefore, $F_0(\tau + \bar{k}M)$ is the Fourier transform of the nondimensionalized pressure jump $[p_0(\bar{x})]$ across the reference (zeroth) blade.

The remaining two boundary conditions that must be satisfied are 1) flow tangency on the blades: for blades undergoing bending and torsional vibrations with amplitudes $\bar{h}_0$ and α_0, referenced to the EA as shown in Fig. 2 of Ref. 1

$$\tilde{v}_0(x) = -ik\bar{h}_0 - [1 + ik(\bar{x} - a)]\alpha_0 \text{ for } |\bar{x}| < 1 \quad (22)$$

and 2) pressure continuity across wakes and ahead of airfoil

$$[\tilde{p}_0(\bar{x})] = 0 \text{ for } |\bar{x}| > 1 \quad (23)$$

Note that because of the manner in which the problem was formulated, these boundary conditions need only be enforced on the zeroth blade and its extension, i.e., $-\infty < \bar{x} < \infty$, $\bar{y} = 0$.

The lift and moment amplitudes can be shown to be directly related to the function $F_0(\tau)$ and its derivative at the point $\tau = \bar{k}M$. To show this, take the inverse Fourier transform of Eq. (20) and observe the pressure continuity boundary

condition, Eq. (23)

$$F_0(\tau)=\frac{1}{2\pi}\int_{-1}^{1}[\bar{p}_0(\bar{x})]\exp[-i(\tau-\bar{k}M)\bar{x}]d\bar{x} \tag{24}$$

Set $\tau=\bar{k}M$ to conclude that the lift amplitude is given by

$$\bar{L}_0=\tilde{L}/(\rho_0U^2b)=-2\pi F_0(\bar{k}M) \tag{25}$$

positive up. Similarly, it is easy to show that the moment amplitude about midchord, positive clockwise, is

$$\bar{M}_{0_{mc}}=\tilde{M}_{mc}/(\rho_0U^2b^2)=2\pi iF_0'(kM) \tag{26}$$

B. Solution Using Discontinuous Integrals

In their treatment of the subsonic problem, Lane and Friedman[13] noted that, if the function $F_0(\tau)$ is taken as an expansion of Bessel functions of integer orders, then the pressure boundary condition $[\bar{p}_0(\bar{x})]=0$ off the airfoil ($|\bar{x}|>1$) is satisfied identically. This is due to the discontinuous nature of the integrals

$$\int_{-\infty}^{\infty}J_n(\tau)e^{i\tau\bar{x}}d\tau,\quad n=0,1,2... \tag{27}$$

which vanish identically for $|\bar{x}|>1$. Lane and Friedman also showed that such a series will satisfy the Kutta condition at the trailing edge and induce the correct leading-edge singularity.

In extending the method to supersonic flow, modifications must be made in order to be consistent with the known characteristics of the supersonic problem. The pressure jump $[\bar{p}_0(\bar{x})]$ need not be zero at the trailing edge and there is no leading-edge singularity, since both edges are assumed supersonic along the entire blade span. This must not be confused with the fact that the leading-edge locus of the cascade is subsonic. Allowances must also be made for the possibility of discontinuities in the pressure distribution along the chord, due to the reflection of Mach waves orginating or being reflected from adjacent airfoils in the cascade. Although it was found numerically expedient to allow for these reflections explicitly in the final solution, this is not a necessary assumption in the development which follows.

In the supersonic case, it is convenient to take the pressure jump as a series of Legendre polynomials

$$[\bar{p}_0(\bar{x})]=\sum_{n=0}^{\infty}p_nP_n(\bar{x}) \tag{28}$$

Such an expansion is justified, since the Legendre polynomials $P_n(\bar{x})$ are complete and form an orthogonal basis on the interval $-1\le\bar{x}\le1$.

When Eq. (28) is substituted into Eq. (24), one obtains

$$F_0(\tau+\bar{k}M)=\frac{1}{2\pi}\sum_{n=0}^{\infty}p_n\int_{-1}^{1}P_n(\bar{x})e^{-i\tau\bar{x}}d\bar{x} \tag{29}$$

The integrals appearing in Eq. (29) can be recognized by setting $\bar{x}=-\cos\bar{\theta}$, then from Ref. 14, page 438, one concludes that

$$\int_{-1}^{1}P_n(\bar{x})e^{-i\bar{x}\tau}d\bar{x}=(-1)^n\int_0^{\pi}P_n(\cos\bar{\theta})e^{i\tau\cos\bar{\theta}}\times\sin\bar{\theta}d\bar{\theta}=\frac{2j_n(\tau)}{i^n} \tag{30}$$

where $j_n(\tau)$ is the spherical Bessel function of the first kind, of order n. Hence, one concludes from Eq. (29) that $F_0(\tau+\bar{k}M)$ may be taken in the form of an infinite series of spherical Bessel functions

$$F_0(\tau+\bar{k}M)=\sum_{n=0}^{\infty}a_nj_n(\tau) \tag{31}$$

where

$$a_n=p_n/(\pi i^n) \tag{32}$$

When this expansion is substituted into the upwash integral equation, Eq. (19), one obtains

$$\bar{v}_0(\bar{x})=\sum_{n=0}^{\infty}a_n\phi_n(\bar{x}) \tag{33}$$

where

$$\phi_n(\bar{x})=\frac{i}{2}\beta\int_{-\infty}^{\infty}G(\tau+\bar{k}M)j_n(\tau)e^{i\bar{x}\tau}d\tau \tag{34}$$

are "shape functions" in the solution of the upwash integral equation. It follows from Eqs. (28-34) that $\pi i^n\phi_n(\bar{x})$ represents the required airfoil vibratory "amplitude shape" $v_0(\bar{x})$ to induce a pressure jump (lift) distribution $P_n(\bar{x})$.

Thus, the problem has been reduced to the determination of the unknown coefficients in Eq. (33). Since the shape functions $\phi_n(\bar{x})$ are not, in general, orthogonal to each other on the interval $-1\le\bar{x}\le1$, one must resort to a numerical procedure. Two such procedures that have proven feasible are both based on a finite number of shape functions, say the first $(N+1)$: $\phi_0,\phi_1,...,\phi_N$. The first procedure is a straight collocation solution of the upwash equation, Eq. (33), where $\bar{v}_0(\bar{x})$ is satisfied at $(N+1)$ discrete points $\bar{x}=\bar{x}_n$; $n=0,1,...,N$. The second procedure is a "best fit" solution of Eq. (33), where the norm $\|\Delta\epsilon\|=(\Delta\epsilon,\Delta\epsilon)^{1/2}$ of the error vector

$$\Delta\epsilon(\bar{x})=\bar{v}_0(\bar{x})-\sum_{n=0}^{N}a_n\phi_n(\bar{x}) \tag{35}$$

is minimized. The inner product $(\cdot,\cdot)$ is defined as

$$(\phi_n,\phi_m)=\int_{-1}^{1}\phi_n(\bar{x})\overline{\phi_m(\bar{x})}d\bar{x} \tag{36}$$

where the bar over $\overline{\phi_m(\bar{x})}$ denotes complex conjugate. By the projection theorem,[15] the solution is simply given by

$$\Delta\epsilon(\bar{x})\perp\phi_n(\bar{x})\ \text{ or }\ (\Delta\epsilon,\phi_n)=0\quad n=0,1,2,...,N \tag{37}$$

that is, the error vector $\Delta\epsilon$ must be orthogonal to each base vector ϕ_n. This leads to $(N+1)$ linear equations in the unknown coefficients $a_0,a_1,...,a_N$. Further details can be found in Ref. 12, where numerically efficient formulas are also obtained for the shape function integrals, Eq. (34), based on the calculus of residues.

C. Mach Wave Reflections

It is advantageous from a numerical standpoint to allow for the reflection of Mach waves in an explicit manner, since they introduce discontinuities in the pressure distribution on the blades. To do this, rewrite the pressure jump $[p_0(\bar{x})]$ across the zeroth blade as follows:

$$[\bar{p}_0(x)]=[\bar{p}_0^s(\bar{x})]+\sum_{r=1}^{N_r}R_r[\bar{p}_0^s(\bar{x}+d_r)]H(\bar{x}-e_r)H(f_r-\bar{x}) \tag{38}$$

where $[\bar{p}_0^s(\bar{x})]$ is now a smooth function, and the sum extends over the reflections possible for the particular cascade geometry and Mach number in question. The unit step functions $H(\bar{x})$ indicate that the rth reflection term is only

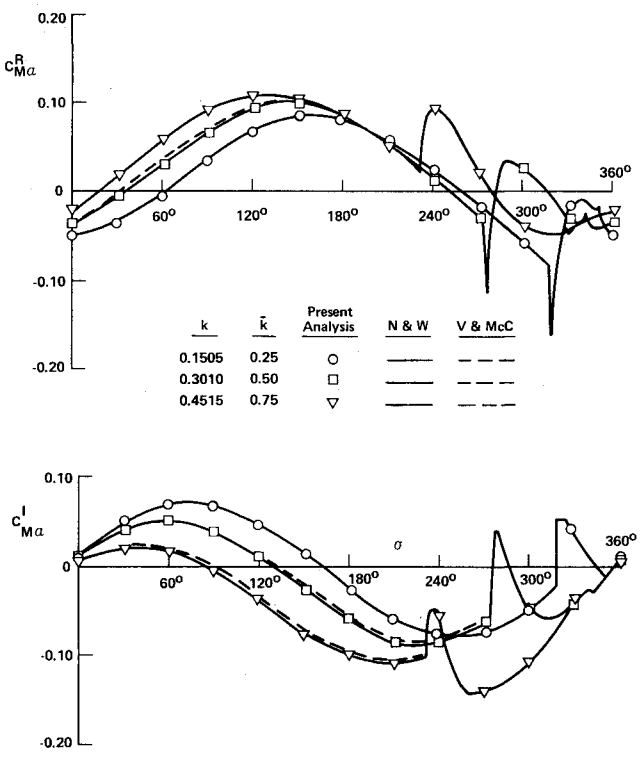

Fig. 2 Comparison of moment coefficient due to torsional oscillations with results of Nagashima and Whitehead,[7] and Verdon and McCune[3]; cascade A, $a=0$.

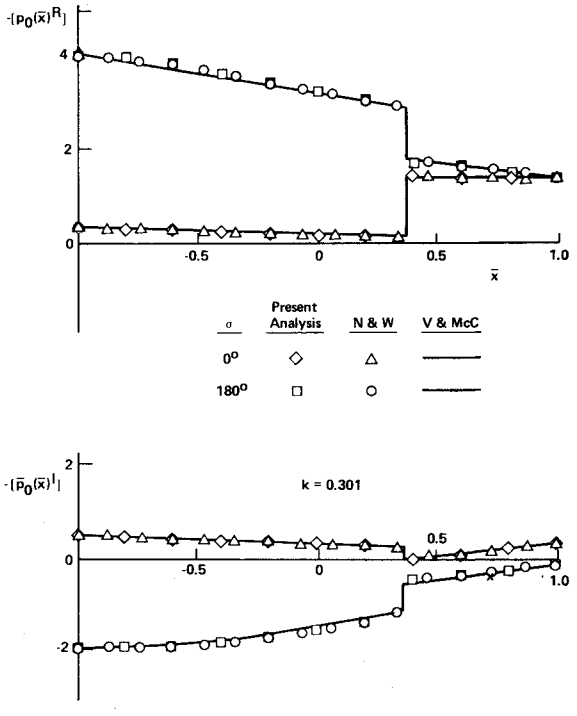

Fig. 3 Comparison of pressure jump amplitude due to torsional oscillations with results of Nagashima and Whitehead,[7] and Verdon and McCune; cascade A, $a=0$.

included if $e_r \leq \bar{x} \leq f_r$, where e_r, f_r, and d_r are constants that depend on the cascade geometry and Mach number. The reflection factor R_r depends not only on geometry and Mach number, but also on the reduced frequency and the interblade phase angle. The derivation of these reflection constants can be found in Ref. 12, together with their numerical values for commonly encountered reflection patterns.

When $[\bar{p}^s_0(\bar{x})]$ is taken as an expansion in terms of Legendre polynomials as before, one obtains

$$\bar{v}_0(\bar{x}) = \sum_{n=0}^{N} a_n \phi^*_n(\bar{x}) \tag{39}$$

where the shape functions $\phi^*_n(\bar{x})$ now account for the reflection terms as well, and are smooth functions of $\bar{x}$.

D. Comparisons with Other Supersonic Theories

To develop confidence in the unsteady aerodynamic theory just described, prior to its application to prediction of elastic stability of cascades, it was subjected to extensive testing. Numerical comparisons were made to results published by Verdon and McCune,[3] Verdon,[4] Nagashima and Whitehead,[7] and Adamczyk and Goldstein,[8] with good agreement obtained in all cases checked.

An illustration of this is presented in Figs. 2 and 3, where results for Verdon's cascade A are compared with computations by Verdon and McCune and Nagashima and Whitehead. The agreement between the present solution and that of Nagashima and Whitehead is excellent, and both agree well with the solution of Verdon and McCune for cascade A. It should be pointed out that Verdon and McCune's solution does not converge for interblade phase angles σ in the super-resonant regime,[3] although this deficiency was later corrected by Verdon's improved solution.[4] Additional comparisons presented in Ref. 12 indicated that the agreement between the present solution and that of Nagashima and Whitehead is excellent also for Verdon's cascade B, but differences are apparent between these solutions and Verdon and McCune's results for low reduced frequency k. Comparisons to the results of Ni[9] were not made, since his paper only presents results for one value of k.

The convergence characteristics of the solution were found to be excellent both for subresonant and super-resonant flows, particularly for the best fit method. It was found that either a seven-point collocation solution, or a best fit solution based on the first seven shape functions, provided more than adequate numerical accuracy and stability for all the flutter calculations. In fact, with as few as three shape functions, solutions typically within 0.2% of the final results are obtained. Execution time per case on the UCLA IBM 3033 computer is about 0.2 s for three shape functions, and about 0.5 s for seven shape functions, using double precision arithmetic. Major improvement in execution time is possible by using single precision arithmetic, since checks have indicated that the loss in accuracy is minimal in the majority of cases. Double precision arithmetic was used throughout this study, however, in order to insure numerical stability in close vicinity of resonance points.

It is interesting to note that the present solution based on the dual integral equation formulation exhibits the same type of resonance phenomenon observed by numerous other investigators.[4,7,16-19]

IV. Method of Solution for the Aeroelastic Eigenvalue Problem

The aeroelastic stability boundaries were obtained using the same procedure (computer program) as used for the incompressible case, and described in Ref. 1. The eigenvalue problem is solved directly, and from the two complex eigenvalues λ_1 and λ_2 two values of the exponent p of the time dependence e^{pt} (previously assumed harmonic $=e^{i\omega t}$) are obtained, where

$$p = (i/\sqrt{\lambda})\omega_T \tag{40}$$

or, in nondimensional form,

$$\bar{p} = p/\omega_T = \bar{p}_R + i\bar{\omega} \tag{41}$$

Table 1 Verdon's cascades A and B

Cascade parameter	Cascade A	Cascade B
Stagger angle	59.5 deg	63.4 deg
Spacing $\bar{s}_2$	0.8	0.6
Mach number M	1.3454	1.2806

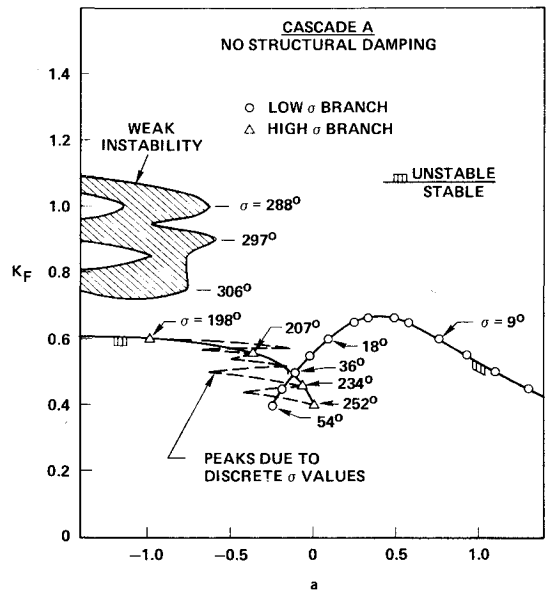

Fig. 4 Critical reduced frequency k_F for SDOF torsional flutter for cascade A.

Flutter occurs when $\bar{p}_R > 0$. The critical interblade phase angle σ is determined by minimizing the flutter speed with respect to σ, while restricting σ to the admissible values $\sigma = 2n\pi/N_b$; $n = 0,1,2,\ldots,N_b - 1$.

The correctness of the flutter boundaries obtained by the preceding procedure was also checked by considering the energy exchange between the cascade and the surrounding airstream.[1]

V. Numerical Results

Two cascade configurations have been studied in depth in Ref. 12, since they cover the practical flow configurations of interest in current design fan blades. Some of the more important results are illustrated in Figs. 4-9. These cascades have also been studied extensively from an aerodynamic standpoint in the publications by Verdon,[3,4] and are often referred to as "Verdon's cascades A and B." The cascade design parameters are shown in Table 1; other pertinent parameters are shown on the figures. In all cases, a titanium rotor with 40 blades and a mass ratio $\mu = 200$ was assumed.

The SDOF torsional flutter boundaries for cascade A are shown in Fig. 4, depicted as the critical reduced frequency k_F at flutter. Although there are certain similarities between this curve and the corresponding one for incompressible flow,[1] there are also some distinct differences. Perhaps the most striking is the appearance of a "bubble" of instability at high reduced frequencies for a torsional axis in the forward region of the chord. As indicated on the figure, this instability is associated with high interblade phase angles, in the supersonic operating regime. The jagged appearance of this bubble is due to the sensitivity of the stability boundary to the interblade phase angle σ. This instability is of a weak kind, associated with a "hump" mode, and is eliminated easily by a small amount of structural damping. It is important to note that similar, weak, instabilities are known to occur also in rotary-wing aeroelasticity.[20]

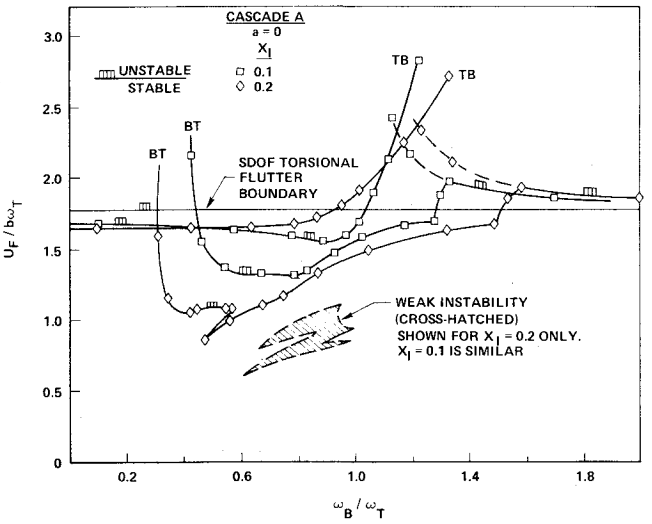

Fig. 5 Coupled bending-torsion flutter boundaries for cascade A, for EA at midchord; $r_\alpha^2 = \frac{1}{3}$, $g_B = g_T = 0$.

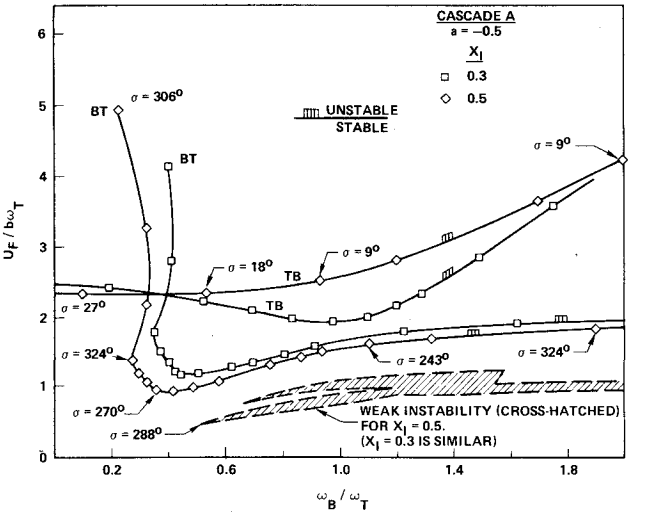

Fig. 6 Coupled bending-torsion flutter boundaries for cascade A, for EA at ¼-chord; $r_\alpha^2 = 0.5833$, $g_B = g_T = 0$.

Stability boundaries for the coupled bending-torsion case, for elastic axis locations at midchord and ¼-chord, respectively, are presented in Figs. 5 and 6. It is quite clear from these figures that the introduction of the bending degree of freedom changes the flutter speed significantly. Because both the bending and the torsional branches exhibit instability over a wide range of frequency ratios, care must be exercised in labeling the branches. It must be kept in mind that the mode shape $\bar{h}_0/\alpha_0$ for a given branch changes as a function of frequency ratio. Therefore, the label BT for "bending-torsion" is used to indicate that bending dominates for low frequency ratios and torsion dominates for high frequency ratios. Conversely, the label TB for "torsion-bending" indicates that the reverse is true; torsion dominates for low frequency ratios and bending dominates for high frequency ratios. Typical values of the interblade phase angle σ at flutter are also shown in Fig. 6. It can be seen that the TB branches have relative low values of σ, whereas BT branches have relatively high values of σ.

There are two interesting differences between the incompressible and the supersonic cascade flutter boundaries. The first is in the behavior of the BT branch, which in the supersonic case shows a marked tendency to become critical for frequency ratios ω_B/ω_T as low as 0.2-0.3. In the incompressible case, the BT branch usually becomes critical only for $\omega_B/\omega_T > 1$, except for negative values of coupling x_α.

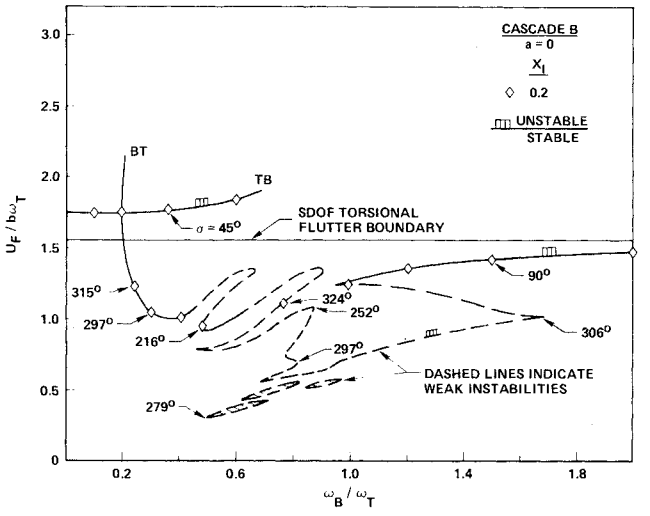

Fig. 7 Coupled bending-torsion flutter boundaries for cascade B, for EA at midchord and no structural damping; $r_\alpha^2 = 1/3$, $g_B = g_T = 0$.

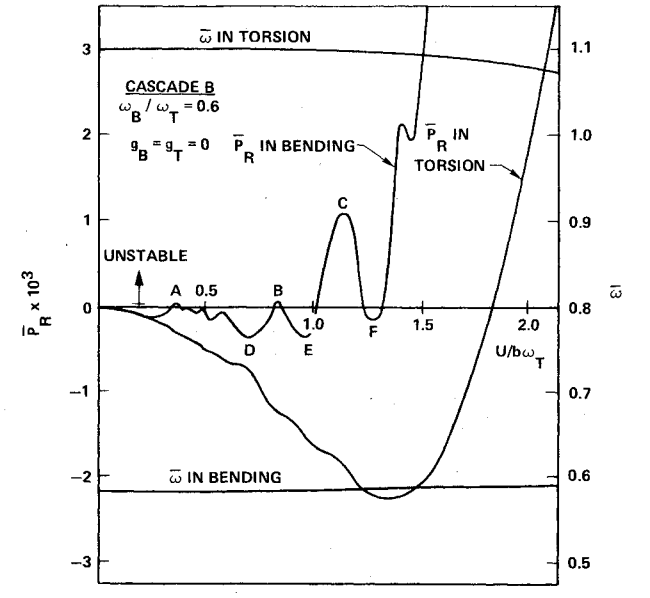

Fig. 8 Frequency and damping vs relative airspeed for cascade B, for EA at midchord; $r_\alpha^2 = 1/3$.

As can be seen from Figs. 5 and 6, this changeover can be very abrupt, indicating a rapid decrease in stability with increasing frequency ratio. For sufficiently low values of ω_B/ω_T, the BT branch becomes susceptible to divergence, although the divergence speed is too high to be of practical importance. The second noticeable difference appears in the form of bubble- and cavity-like regions of weak instability. They are due to the presence of humps, i.e., local maxima and minima, in the damping vs airspeed plot of the BT mode, and are eliminated when small amounts of structural damping are introduced.

The stability boundaries of cascade B for the coupled bending-torsion case are shown in Figs. 7-9. Although similarities exist between these results and the corresponding ones already presented for cascade A, certain new features occur that are due to the differences in the flow configurations represented by the two cascades. In Fig. 7, which represents the case of EA at midchord and a coupling strength $x_I = 0.2$, several regions of both weak instability and weak stability occur. The weak instabilities are represented by three small bubbles, and a large plus several smaller cavities, while the weak stabilities manifest themselves as fingerlike extensions, usually separated by narrow regions of weak instability.

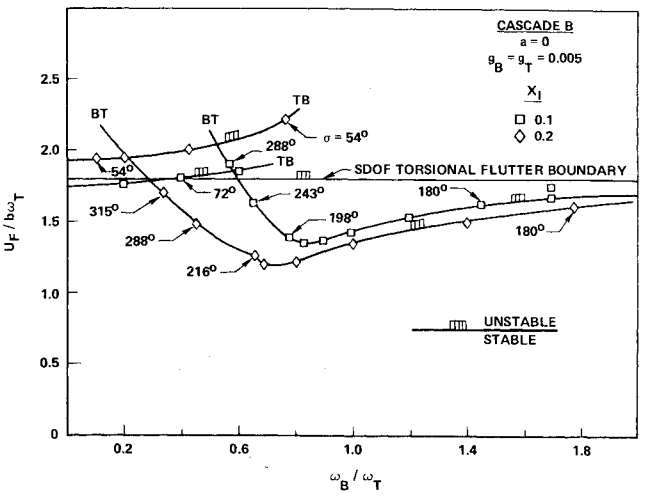

Fig. 9 Effect of structural damping on flutter boundaries for cascade B, for EA at midchord; $r_\alpha^2 = 1/3$, $g_B = g_T = 0.005$.

The reason for this map-like appearance of the flutter boundaries can be traced to the appearance of multiple humps in the damping vs $U/b\omega_T$ plot of the bending mode, as illustrated in Fig. 8. The strikingly oscillatory behavior of the damping in bending, represented by the real part $\bar{p}_R$ of the exponent p, together with a relatively low level of damping in this mode, results in several local maxima of the $\bar{p}_R$ vs $U/b\omega_T$ plot. Three of these, labeled A, B, and C, lie in unstable regions. Neutral stability, i.e., the flutter boundary, is represented by the points $U_F/b\omega_T$ where the $\bar{p}_R$ vs $U/b\omega_T$ plot crosses the $U/b\omega_T$ axis. If the slope of the curve is positive at such a cross-over point, the corresponding point on the flutter boundary separates a stable region below (lower $U/b\omega_T$) from an unstable region above (high $U/b\omega_T$). If, on the other hand, the slope is negative, the reverse is true; that is, the region above the point is stable and the region below is unstable.

In the latter case, where the $\bar{p}_R$ vs $U/b\omega_T$ slope is negative when $\bar{p}_R = 0$, certain anomalies in the system behavior will occur. One such anomaly is the fact that at such a point, the system goes unstable if the relative airspeed $U/b\omega_T$ is lowered, or, what is effectively the same, if the reduced frequency k is increased. Increasing the speed or reducing the frequency k stabilizes the system, provided the change is small. Clearly, if the change in $U/b\omega_T$ is large enough, the system will pass straight through the stable region and eventually enter another region of instability.

A second and equally interesting anomaly occurs when damping is introduced. The fingerlike regions of weak stability disappear, and damping is then seen to be destabilizing for a cascade operating in these regions. Introduction of damping typical of fan rotors, $g_B = g_T = 0.005$ ($\delta \simeq 0.015$), also eliminates the regions of weak instability, leaving the flutter boundaries reasonably smooth, as shown in Fig. 9. But also note that the bending-torsion (BT) branch instability persists, lowering the flutter speed significantly below the SDOF torsional value, over a wide range of frequency ratios ω_B/ω_T. Increasing the coupling strength x_I from 0.1 to 0.2 moves the BT branch down and to the left, bringing the minimum of the curve from a frequency ratio of about 0.82 to a ratio of about 0.72. The corresponding decrease in the flutter speed $U_F/b\omega_T$ at the minimum is approximately 11%. It should also be noted that a considerable number of additional results can be found in Refs. 12 and 21.

Finally, an interesting observation regarding the predicted characteristics of instabilities of the bending mode should be mentioned. It is clear from Figs. 5-9 that this type of instability is a real possibility in the supersonic case for frequency ratios in the practical range $0.3 < \omega_B/\omega_T < 0.8$. Since the bending branch frequency has been found extremely insensitive to relative airspeed, cf. Fig. 8, the flutter frequency would be very close to the natural frequency of the bending

mode in vacuum. It is interesting to note that this is predicted to be a low k, high σ type flutter—a characteristic which it has in common with the shock-induced bending flutter predicted by the theory of Goldstein et al.[22]

VI. Conclusions

The major conclusions that can be drawn from this study are summarized in the following. They should be considered as indicative of trends, but must be interpreted in the light of the assumptions and models used in this study. The extension of this analysis to a more sophisticated structural model offers no conceptual difficulty, and is a logical next step toward a better understanding of flutter in fan and compressor blading.

1) The effect of coupling between the bending and torsional degrees of freedom significantly changes the stability boundaries of a typical cascade.

2) There is no appreciable tendency for the bending and torsional frequencies to coalesce as flutter is approached, except at very low reduced frequencies.

3) The supersonic flutter problem is strongly influenced by the cascade flow configuration, particularly the Mach wave reflection pattern.

4) The bending branch often appeared as a hump mode, resulting in both bubble-like regions of weak instability as well as finger-like regions of weak stability. Both were found to disappear when structural damping of the order of 1.5% of critical was introduced.

5) Structural damping has a pronounced beneficial effect on the flutter boundaries, except in the regions of weak stability, where damping often is destabilizing.

6) The results indicate that the bending branch is often the critical mode, even in the absence of finite mean lift or incidence, or strong shocks in the blade passages.

7) The unsteady supersonic aerodynamic theory for cascades developed in this study was found to be computationally efficient and well suited for incorporation in the general flutter prediction system used to treat the coupled bending-torsion problem.

References

[1] Bendiksen, O. and Friedmann, P., "Coupled Bending-Torsion Flutter in Cascades," *AIAA Journal*, Vol. 18, Feb. 1980, pp. 194-201; also presented as AIAA Paper 79-0793 at the AIAA/ASME/ASCE/AHS 20th Structures, Structural Dynamics and Materials Conference, St. Louis, Mo., April 4-6, 1979.

[2] Whitehead, D. S., "Force and Moment Coefficients for Vibrating Aerofoils in Cascade," Great Britain Aeronautical Research Council, R&M 3254, 1960.

[3] Verdon, J. M. and McCune, J. E., "Unsteady Supersonic Cascade in Subsonic Axial Flow," *AIAA Journal*, Vol. 13, Feb. 1975, pp. 193-201.

[4] Verdon, J. M., "Further Developments in the Aerodynamic Analysis of Unsteady Supersonic Cascades, Parts 1 and 2," *Journal of Engineering for Power, Transactions of the ASME*, Ser. A., Vol. 99, Oct. 1977, pp. 509-525.

[5] Kurosaka, M., "On the Unsteady Supersonic Cascade with a Subsonic Leading Edge—An Exact First Order Theory: Parts 1 and 2," *Journal of Engineering for Power, Transactions of the ASME*, Ser. A, Vol. 96, Jan. 1974, pp. 13-31.

[6] Brix, C. W. and Platzer, M. F., "Theoretical Investigation of Supersonic Flow Past Oscillating Cascades with Subsonic Leading-Edge Locus," AIAA Paper 74-14, 1974.

[7] Nagashima, T. and Whitehead, D. S., "Linearized Supersonic Unsteady Flow in Cascades," Great Britain Aeronautical Research Council, R&M 3811, 1978.

[8] Adamczyk, J. J. and Goldstein, M. E., "Unsteady Flow in a Supersonic Cascade with Subsonic Leading-Edge Locus," *AIAA Journal*, Vol. 16, Dec. 1978, pp. 1248-1254.

[9] Ni, R. H., "A Rational Analysis of Periodic Flow Perturbation in Supersonic Two-Dimensional Cascade," ASME Paper 78-GT-176, April 1978.

[10] Lane, F., "System Mode Shapes in the Flutter of Compressor Blade Rows," *Journal of the Aeronautical Sciences*, Vol. 23, Jan. 1956, pp. 54-66.

[11] Miles, J. W., *The Potential Theory of Unsteady Supersonic Flow*, Cambridge University Press, Cambridge, Great Britain, 1959.

[12] Bendiksen, O. O., "Coupled Bending-Torsion Flutter in Cascades with Applications to Fan and Compressor Blades," Ph.D. Dissertation, Mechanics and Structures Dept., Univ. of Calif., Los Angeles, March 1980; also available as UCLA Rept. ENG-8072, July 1980.

[13] Lane, F. and Friedman, M., "Theoretical Investigation of Subsonic Oscillatory Blade-Row Aerodynamics," NASA TN-4136, Feb. 1958.

[14] Abramowitz, M. and Stegun, I. A., eds., *Handbook of Mathematical Functions*, NBS Applied Mathematics Series 55, U.S. Government Printing Office, Washington, D.C., 1965.

[15] Naylor, A. W. and Sell, G. R., *Linear Operator Theory in Engineering and Science*, Holt, Reinhart and Winston, Inc., New York, 1971, pp. 297-305.

[16] Samoilovich, G. S., "Resonance Phenomena in Sub- and Supersonic Flow Through an Aerodynamic Cascade," *Mekhanika Zhidkosti i Gaza*, Vol. 2, May-June 1967, pp. 143-144.

[17] Kurosaka, M., "On the Issue of Resonance in an Unsteady Supersonic Cascade," *AIAA Journal*, Vol. 13, Nov. 1975, pp. 1514-1516.

[18] Verdon, J. M., "Comment on 'On the Issue of Resonance in an Unsteady Supersonic Cascade,' " *AIAA Journal*, Vol. 13, Nov. 1975, pp. 1542-1543.

[19] Runyan, H. L., Woolston, D. S., and Rainey, A. G., "Theoretical and Experimental Investigation of the Effect of Tunnel Walls on the Forces on an Oscillating Airfoil in Two-Dimensional Subsonic Compressible Flow," NACA TN-3416, 1955.

[20] Friedmann, P., "Recent Developments in Rotary-Wing Aeroelasticity," *Journal of Aircraft*, Vol. 14, Nov. 1977, pp. 1027-1041.

[21] Bendiksen, O. and Friedmann, P., "Coupled Bending-Torsion Flutter in a Supersonic Cascade," AIAA Paper 80-0701, Seattle, Wash., 1980.

[22] Goldstein, M. E., Braun, W., and Adamczyk, J. J., "Unsteady Flow in a Supersonic Cascade with Strong In-Passage Shocks," *Journal of Fluid Mechanics*, Vol. 83, Nov. 1977, pp. 569-604.